Molecular Biology of the Cell
Vol. 15, 332–344, January 2004

A General Role for Rab27a in Secretory Cells[D][V]

Tanya Tolmachova,* Ross Anders,* Jane Stinchcombe,† Giovanna Bossi,† Gillian M. Griffiths,† Clare Huxley,* and Miguel C. Seabra*‡

*Cell and Molecular Biology, Division of Biomedical Sciences, Faculty of Medicine, Imperial College London, London SW7 2AZ, United Kingdom; and †Sir William Dunn School of Pathology, University of Oxford, Oxford OX1 3RE, United Kingdom

Submitted July 1, 2003; Revised October 2, 2003; Accepted October 3, 2003
Monitoring Editor: Jean Gruenberg

Vesicular transport is a complex multistep process regulated by distinct Rab GTPases. Here, we show for the first time that an EGFP-Rab fusion protein is fully functional in a mammalian organism. We constructed a PAC-based transgenic mouse, which expresses EGFP-Rab27a under the control of endogenous *Rab27a* promoter. The EGFP-Rab27a transgene was fully functional and rescued the two major defects of the *ashen* Rab27a knockout mouse. We achieved cell-specific expression of EGFP-Rab27a, which faithfully followed the pattern of expression of endogenous Rab27a. We found that Rab27a is expressed in an exceptionally broad range of specialized secretory cells, including exocrine (particularly in mucin- and zymogen-secreting cells), endocrine, ovarian, and hematopoietic cells, most of which undergo regulated exocytosis. We suggest that Rab27a acts in concert with Rab3 proteins in most regulated secretory events. The present strategy represents one way in which the complex pattern of expression and function of proteins involved in specialized cell types may be unraveled.

INTRODUCTION

Rab27a is a member of a large family of Ras-related small GTPases. Rabs have distinct subcellular localizations and are believed to regulate specific steps in intracellular traffic (Pfeffer, 2001; Segev, 2001; Zerial and McBride, 2001; Goud, 2002; Seabra *et al*., 2002). A recent genome analysis revealed that the Rab family is composed of 11 members in *Saccharomyces cerevisiae*, 7 in *Schizosaccharomyces pombe*, 29 in both *Caenorhabditis elegans* and *Drosophila melanogaster*, and 60 in *Homo sapiens* (Pereira-Leal and Seabra, 2001).

Rab27a is unique at present because it is the only known Rab associated with disease in humans (Seabra *et al*., 2002). Loss-of-function mutations in the *RAB27A* gene result in Griscelli syndrome, which is a rare autosomal disorder characterized by partial cutaneous albinism and immunodeficiency due to failure of cytotoxic T lymphocytes (CTLs) to secrete the contents of their lytic granules (Menasche *et al*., 2000; Bahadoran *et al*., 2001). A natural mouse mutant, *ashen* (*Rab27a*^{ash}), has a mutation in *Rab27a* and exhibits the same phenotypic features as Griscelli syndrome patients (Wilson *et al*., 2000; Haddad *et al*., 2001; Hume *et al*., 2001; Stinchcombe *et al*., 2001; Wu *et al*., 2001). Recent studies suggest that Rab27a is associated with melanosomes in pigmented cells and regulates melanosome transport via its interaction with actin-based cellular motors such as myosin Va and myosin VIIa (Hume *et al*., 2001, 2002; Wu *et al*., 2001; El-Amraoui *et al*., 2002; Provance *et al*., 2002; Wu *et al*., 2002). Myosin Va and myosin VIIa do not interact directly with Rab27a but require linker proteins, melanophilin and Myrip, respectively, that bind GTP-bound Rab27a through a conserved N-terminal domain, and myosins through a medial domain (El-Amraoui *et al*., 2002; Fukuda *et al*., 2002b; Strom *et al*., 2002; Wu *et al*., 2002).

Rab27a is also required for secretion of lytic granules in CTLs (Menasche *et al*., 2000; Haddad *et al*., 2001; Stinchcombe *et al*., 2001). In *ashen* mice, lytic granules polarize correctly toward target cells but are unable to kill due to impaired secretion of their granules (Stinchcombe *et al*., 2001). The role of Rab27a in lytic granule secretion is independent of myosin Va or melanophilin, suggesting that Rab27a might interact with other effector proteins in different cell types (Hume *et al*., 2002). Consistently, a new family of Rab27 effector proteins has been recognized recently and includes JFC1/Slp1, Slp2a, Slp3a, granuphilin/Slp4, Slp5, and Slac2b in addition to melanophilin and Myrip (El-Amraoui *et al*., 2002; Kuroda *et al*., 2002a,b; Strom *et al*., 2002; Yi *et al*., 2002).

Melanosomes and CTLs are only a subset of cell types expressing Rab27a. Previous studies using immunoblot analysis indicated that the Rab27a protein is expressed widely in the hematopoietic lineage, spleen, lung, eye, pancreas, and the gastrointestinal tract (Seabra *et al*., 1995; Barral *et al*., 2002). Other tissues such as liver, heart, muscle, testis, and brain show little, if any, expression of Rab27a when tissues are properly perfused (Seabra *et al*., 1995; Barral *et al*., 2002). In addition, recent studies suggest a role for Rab27a in exocytosis of insulin and chromaffin granules in endocrine cells (Fukuda *et al*., 2002a; Yi *et al*., 2002). The cell type expression of Rab27a within these tissues, its subcellular localization, and mechanism of action in these cell types remain unknown. In this work, we constructed a mouse model that expresses tissue- and cell-specific Rab27a fused to enhanced green fluorescent protein (EGFP). Our analysis suggests a previously unsuspected wide role for Rab27a in nonneuronal regulated-secretory cells.

Article published online ahead of print. Mol. Biol. Cell 10.1091/mbc.E03–07–0452. Article and publication date are available at www.molbiolcell.org/cgi/doi/10.1091/mbc.E03–07–0452.

[D] [V] Online version of this article contains videos and supplementary figures. Online version available at www.molbiolcell.org.

‡ Corresponding author. E-mail address: m.seabra@imperial.ac.uk.

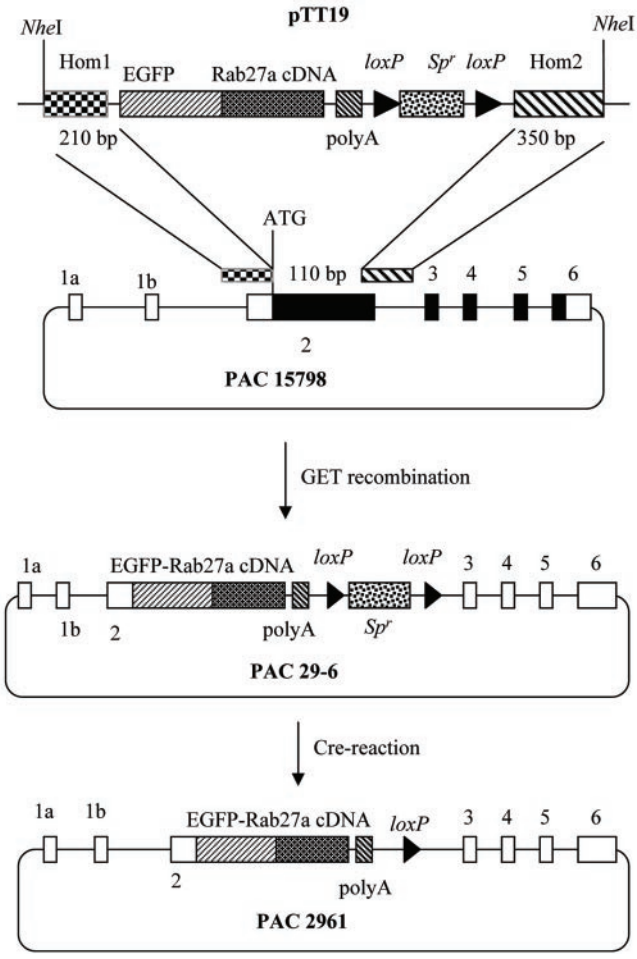

Figure 1. Construction of a PAC containing the EGFP-Rab27a fusion gene under the control of the *RAB27A* promoter by homologous recombination in *E. coli*. PAC15798 contains human *RAB27A* gene, where coding/noncoding exons are represented by filled/open rectangles, respectively. The insertion of EGFP-Rab27a cassette as an *Nhe*I fragment from pTT19 into PAC15798 by homologous recombination is described under MATERIALS AND METHODS.

MATERIALS AND METHODS

Construction of Plasmid pTT19

The targeting plasmid pTT19 was used to introduce the EGFP-Rab27a gene into PAC 15798 (Tolmachova *et al*., 1999) (Figure 1). Plasmid pTT19 contains an EGFP-Rab27a fusion mini-gene followed by a polyA sequence, a spectinomycin (Sp) resistance gene (*Sp*^{r}) to serve as a selectable marker for recombination flanked by *loxP* sites (to allow it to be removed from the PAC after modification), and two homology sequences on the left and right arms to promote homologous recombination (Figure 1). These sequences were flanked by two *Nhe*I-sites to isolate a 4.4-kb fragment exposing the 5′- and 3′-homology fragments at the ends. The construction of plasmid pTT19 proceeded as follows. The 5′-homology fragment (Hom1) was obtained as a 210-base pair polymerase chain reaction (PCR) product with an *Nhe*I site introduced into the 5′ end by using the following primers: forward primer 5′-GGCTAGCTTCTCATCTAGCTAGTTATTAGG and reverse primer 5′-AACCGGTAATGAAGAACTCAGTAGTTCACC. *Taq*I polymerase was inactivated by phenol-chloroform extraction, and the PCR product was blunt-ended with the Klenow subunit of polymerase I. It was then cloned into the blunt-ended *Nhe*I site of plasmid pEGFPRab27a, which contains an EGFP-Rab27 fusion protein followed by a polyA addition signal (Hume *et al*., 2001). The *Kpn*I site in plasmid pDLox3 [a gift from O. Tolmachov (Bigger *et al*., 2001)] was changed into a *Not*I site. The resulting plasmid pDLox4 contains two *loxP* sites in the same orientation, separated by several cloning sites (including *Hin*dIII) and flanked by two *Not*I sites. The spectinomycin resistance gene (*Sp*^{r}) was isolated from the plasmid pWM5 [a gift from B. Wanner (Metcalf and Wanner, 1993)] as a 2-kb *Hin*dIII fragment and subcloned into the *Hin*dIII site of pDLox4. The resulting plasmid pDLox5 contains two *loxP* sites separated by the selectable marker *Sp*^{r}, flanked by two *Not*I sites (Supplemental Figure S1). The 3′-homology fragment (Hom2) was generated as a 350-base pair fragment by PCR (forward primer 5′-TTATCACAACAGTGGGCATTGATTTCAGGG and reverse primer 5′-AACGCGTGCTAGCAGGCTTCAAGACAAAGG) and cloned into pGEM-T (Stratagene, La Jolla, CA). During PCR, *Nhe*I and *Mlu*I sites were introduced at the 3′ end of Hom2. The resulting plasmid pGEMT-Hom2 has a single *Not*I site 5′ of Hom2 into which the 2.1-kb *Not*I fragment of pDLox5 containing *loxP*- *Sp*^{r}-*loxP* was inserted. The resulting plasmid pGEMT-Hom2*Sp* was digested with *Mlu*I and the 2.5-kb fragment containing *loxP*-*Sp*^{r}-*loxP*-Hom2 was cloned into the *Mlu*I site of plasmid pEGFPRab27aHom1 3′ of the polyA sequence.

Modification of PAC 15798 Containing the RAB27A Gene

The EGFP-Rab27a cDNA was introduced into the PAC 15798 by GET recombination, i.e., homologous recombination in *Escherichia coli* induced by the *g*am, *recE*, and *recT* genes contributed by the plasmid pGETrec (Narayanan *et al*., 1999). First, plasmid pGETrec (a gift from P.A. Ioannou, Murdoch Children's Research Institute, Royal Children's Hospital, Melbourne, Australia) was electroporated into the *E. coli* strain containing PAC 15798. To prepare electrocompetent cells, 1 ml of overnight culture grown in LB with 25 μg/ml kanamycin (Km) was seeded into fresh LB/Km at a ratio of 1:100 and grown for 4–5 h at 37°C with shaking. Cells were centrifuged at 5000 rpm for 10 min at 4°C and washed twice with ice-cold 10% glycerol. The pellet was resuspended in 50 μl of ice-cold 10% glycerol, and for each electroporation 30–50 μl of cells and 10 ng of DNA were used. Electroporation conditions were 1.8 kV, 200 Ω, 25 μF in a 0.1-cm electrode gap cuvette (Bio-Rad, Hercules, CA). Cells were grown in LB for 2 h at 37°C with shaking before being plated on LB/ampicillin (100 μg/ml)/Km (25 μg/ml) plates. The 4.4-kb *Nhe*I fragment from pTT19 containing the EGFP-Rab27A cassette (Figure 1) was gel-purified using the QIAEX II gel extraction kit (QIAGEN, Valencia, CA). Electrocompetent cells were prepared from *E. coli* containing PAC15798 and pGETrec as described above except that after seeding the overnight culture into LB/Km/ampicillin and culturing for 3 h, 10% L-arabinose was added to the cells to a final concentration of 0.2% to induce the arabinose-inducible P_{BAD} promoter. Cells were cultured for 40 min at 37°C in the presence of 0.2% L-arabinose, then spun at 5000 rpm for 10 min at 4°C and washed twice with ice-cold 10% glycerol. The pellet was resuspended in ice-cold 10% glycerol and electroporated (40 μl of cells) with the 4.4-kb *Nhe*I-fragment containing the EGFP-Rab27A cassette (100–500 ng) under the conditions described above. Cells were grown for 3 h at 37°C with shaking and then plated on LB/Km (25 μg/ml)/Sp (25 μg/ml). Colonies were screened directly by PCR by using buffer A (10 mM Tris-HCl, pH 8.3, 50 mM KCl, 2 mM $MgCl_2$) and primers to check correct integration at the 5′ end: forward primer to the 5′ outside the region of homology Hom 1 (5′-CTCCCAAAGTGCTGGGATTACCTGTGTGTT) and reverse primer in the EGFP region (5′-AGTCGTGCTGCTTCATGTGG). The correct product of 550 base pairs was detected in 20 of 38 clones. Positive colonies were screened by PCR to check for correct integration at the 3′ end by using a forward primer in the *Sp*^{r} gene (5′-TTTGCAACTGCGGGTCAAGG) and a reverse primer to the 3′ end outside the region of homology Hom2 (5′-CAAGAGTATGAGGGGCAAGG). All 20 clones produced the correct size 700-base pair band. Four positive clones were checked by restriction analysis using *Not*I. The modified PAC was named PAC 29-6 (Figure 1). The *Sp*^{r} gene was removed from PAC 29-6 by using arabinose inducible Cre recombinase encoded by plasmid pBAD75Cre, which has a temperature-sensitive origin of replication [a gift from B. Bigger (Bigger *et al*., 2001)]. Electrocompetent cells containing PAC 29-6 were electroporated with pBAD75Cre as described above, and the cells plated out on LB/chloramphenicol (Cm) (30 μg/ml)/Sp (25 μg/ml)/0.5% glucose at 30°C. A single resulting colony was seeded into 5 ml of LB/Cm(30 μg/ml)/Sp (25 μg/ml)/0.5% glucose, grown overnight at 30°C, spun at 5000 rpm for 10 min, resuspended in 5 ml of LB/0.5% L-arabinose, and then grown for 5 h at 30°C with shaking. The cells were spread on LB/Km (25 μg/ml) plates and grown at 42°C overnight. The colonies were streaked on LB/Km, LB/Sp, and LB/Cm plates. Clones with $Km^rCm^sSp^s$ phenotype were checked by PCR by using one primer in the Rab27a cDNA (5′-TTGAGATGCTTCTGGACCTGATAATGAA) and the other in the 3′ end of Hom2 (5′-AACGCGTGCTAGCAGGCTTCAAGACAAAGG). Three positive clones yielding the correct size 900-base pair fragment were checked by restriction analysis by using *Cla*I and *Nru*I. The modified PAC was named PAC 2961 (Figure 1).

Mouse Stocks, Generation of Transgenic Mice, and Genotyping

All mice were bred and maintained under UK project license PPL 70/5071 at the Central Biomedical Services of Imperial College, London. C57BL/6J and C3H/He wild-type mice were purchased from B&K Universal Limited (Hull, United Kingdom). Our colonies of *ashen* mice (C3H/HeSn-*ash*/*ash* and C57BL/6J-*ash*/*ash*) have been described previously (Barral *et al*., 2002). Statistical analysis of litter sizes was performed using analysis of variance. DNA of modified PAC 2961 was isolated using Plasmid Maxi kit (QIAGEN) and microinjected at low concentration (0.5–1 ng/μl) into mouse pronuclei in

Table 1. Primers for amplification of the exons of the human *RAB27A* gene

Exon	Size of PCR product (bp)	Forward primer	Reverse primer
1a	300	5′-cttgactggtctgcagtgcc	5′-tttacagggtagagaaccgc
1b	100	5′-gaaacctggaaatctaaggc	5′-gtcaagcagagctgggtttg
4	385	5′-aggtttcgtagcttaacgacagcgttcttc	5′-ataagagtctcttctgtggg
5	240	5′-gcatattgtgaaaacccagatatagtgctg	5′-ggacacattcaacatgcccc
6	420	5′-ttgagatgcttctggacctgataatgaa	5′-ctgaatccttgaatgatttactataatagg

(C57BL/6J × CBA/Ca) F2 oocytes that were implanted into foster females by using standard techniques (Hogan *et al*., 1994). Offspring resulting from these injections were weaned and genotyped by PCR at 3 wk of age. DNA was isolated from 1-mm tail biopsy by digestion in 200 μl of buffer B (50 mM KCl, 1.5 mM $MgCl_2$, 10 mM Tris-HCl, pH 8.5, 0.01% gelatin, 0.45% Nonidet P-40, 0.45% Tween 20) supplemented with 50 μg/ml Proteinase K (Sigma-Aldrich, St. Louis, MO) at 55°C overnight. The Proteinase K was inactivated by heating at 95°C for 15 min. The tubes were spun at 14,000 × *g* for 5 min and 2 μl of supernatant were used to perform a 10-μl PCR reaction in buffer C (10 mM Tris-HCl, pH 8.3, 50 mM KCl, 1 mM $MgCl_2$). For identification of transgene-positive mice, we used primers JR62 and JR63 specific for rat Rab27a cDNA (Ramalho *et al*., 2002). Cycling conditions were 94°C for 3 min, followed by 32 cycles of 94°C for 40 s, 62°C for 40 s, 72°C for 1 min, and finally 72°C for 10 min. PCR analysis using pairs of primers specific for sequences outside human *RAB27A* gene exons (Table 1) was used to verify that transgenic founders FR82, 84, and 90 contained the entire PAC 2961. The PCR cycling conditions were as described above, except 30 cycles for positive control (DNA of PAC 2961).

Immunoblotting

Frozen tissues were thawed, resuspended in lysis buffer D (50 mM HEPES, pH 7.2, 10 mM NaCl, 1 mM dithiothreitol, 0.5 mM phenylmethylsulfonyl fluoride, 5 μg/ml pepstatin, 5 μg/ml aprotinin, 5 μg/ml leupeptin) (Sigma-Aldrich) and mechanically disrupted using a Polytron homogenizer. Homogenates were spun at 7000 × *g*, 10 min at 4°C. The postnuclear supernatant was collected, and protein concentration was determined using Coomassie Plus protein assay reagent (Pierce Chemical, Rockford, IL). Equal amounts of total protein (50 μg) were subjected to SDS-PAGE on 12% acrylamide gels and transferred to Immobilon-P transfer membrane (Millipore, Bedford, MA). The membranes were dried overnight, blocked with 5% skimmed milk in phosphate buffer saline supplemented with 0.1% Tween 20 for 1 h and incubated with monoclonal anti-rat Rab27a antibody 4B12 (Hume *et al*., 2001) or polyclonal anti-calnexin antibody (Stressgen Biotechnologies Corp., Victoria, British Columbia, Canada) diluted 1:10,000. Filters were washed three times with phosphate buffer saline supplemented with 0.1% Tween 20 for 15 min, incubated with secondary antibody, washed again as described above, and developed using SuperSignal West Pico Chemiluminescence Substrate (Pierce Chemical).

Tissue Histology and Immunohistochemistry

Mice were perfused with phosphate-buffered saline (PBS), organs were fixed with 4% paraformaldehyde in PBS at 4°C overnight (1 h for the eye), kept in 20% sucrose in PBS at 4°C overnight, and imbedded in OCT compound (BDH, Poole, Dorset, United Kingdom) by using an isopentane-liquid nitrogen bath. The tissues were sliced at 7-μm thickness, mounted in Vectashield mounting medium (Vector Laboratories, Burlingame, CA), and examined using a DM-IRBE confocal microscope (Leica, Wetzlar, Germany). Lenses used were PL Fluotar 40 ×/1.00 (oil) and PL APO 100 ×/1.40 (oil). Images were processed using Leica-TCS-NT software and Leica Confocal Software associated with microscope, Adobe Photoshop 5.5 software and Microsoft PowerPoint software. All images presented are single sections on the z-plane. All images shown are merged pictures of sections excited with 488 nm to elicit EGFP-Rab27a fluorescence and 568 nm to elicit intrinsic autofluorescence observed in most tissues. On merged images EGFP signal is green, whereas autofluorescence is yellow or red.

For immunohistochemistry of the pancreas, the tissue was fixed and frozen as described above and cut at 7-μm thickness. Sections were rehydrated in PBS twice for 10 min and blocked in buffer E (1 × PBS, 1% bovine serum albumin [BSA], 0.2% Triton X-100, 10% mouse serum, 10% goat serum) for 30 min at room temperature. The sections were incubated with rabbit anti-glucagon antibody (Chemicon International, Temecula, CA) or guinea pig anti-insulin antibody (DAKO, Carpinteria, CA) in buffer E overnight and then washed in PBS twice for 10 min. After staining with appropriate secondary Alexa-568–conjugated antibody for 40 min in buffer E, the sections were washed in PBS twice for 10 min, mounted in Vectashield medium (Vector Laboratories), and examined using a DM-IRBE confocal microscope (Leica).

Cell Culture

CTLs were derived as described previously (Stinchcombe *et al*., 2001). In brief, 2.5 × 10^6 splenocytes from the effector strain (*ash/ash*, *ash/+*, or *ash/ash*,Tg) were activated with 2.5 × 10^6 irradiated (3000 rad) stimulator splenocytes from BALB/c mice in 10 ml of DMEM containing 7% heat-inactivated fetal calf serum (FCS), 50 μM 2-mercaptoethanol, and antibiotics. After 5 d in culture at 37°C with 10% CO_2, CTLs were purified over Histopaque-1083 (Sigma-Aldrich), washed with PBS resuspended in culture medium supplemented with 100 U/ml interleukin-2. CTLs were restimulated after 7 d with the same number of irradiated stimulator splenocytes.

Cytotoxicity Assay

Cytotoxicity was assayed using a Cytotox 96 nonradioactive kit (Promega, Madison, WI) following the manufacturer's instructions. Briefly, Ficoll-purified T-cells were plated in 96-well plates at the effector/target ratios shown using 10^4 P815 (H2d) target cells per well in a final volume of 100 μl per well by using RPMI lacking phenol red. Lactate dehydrogenase release, indicative of target cell lysis, was assayed after 4-h incubation at 37°C by removal of 50-μl aliquots of supernatant from each well and incubation with appropriate substrate for 30 min and the absorbance read at 490 nm as described previously (Stinchcombe *et al*., 2001).

Live Cell Video Microscopy

CTLs derived from transgenic mice expressing EGFP-Rab27a (*ash/ash*,Tg^{FR84}) were grown in the presence of 60 nM LysoTracker red DND-99 (Molecular Probes, Eugene, OR) for 2 h at 37°C in RPMI, 10% FCS, followed by washing three times in PBS and resuspending in 100 ml of RPMI, 10% FCS. P815 targets cells were allowed to adhere on a glass coverslip mounted in a temperature-controlled chamber for 10 min at 37°C in RPMI without phenol red and serum. FCS was restored to the medium to a final concentration of 10% FCS. The LysoTracker Red DND-99–loaded CTLs were added to the P815 in the chamber. Sequential confocal images were acquired every 30 s. A Nikon TE300 microscope attached to a Bio-Rad Radiance 2000 MP laser scanning microscope was used, with 488-nm and 543-nm laser epifluorescence and Nomarski differential interference contrast for the transmitted light. The images were processed using MetaMorph version 4.5 software.

Electron Microscopy

CTLs prepared from FR84-rescued *ashen* spleens were incubated with horseradish peroxidase to label secretory lysosomes, conjugated to P815 target cells, and plated as described previously (Stinchcombe *et al*., 2001). Briefly, 5–7 d after activation CTLs were incubated at 37°C overnight with 2 mg/ml horseradish peroxidase (Roche Diagnostics, Indianapolis, IN) added directly to the growth medium then washed three to four times by pelleting and resuspension in RPMI, and the final cell pellet resuspended to a concentration of ~1–5 × 10^6 cells/ml in RPMI. CTLs were then mixed 1:1 with P815 target cells (washed once and resuspended to concentration of ~1–5 × 10^6 cells/ml in RPMI), the mixture left for 5 min in suspension, and then plated in 12-well plastic dishes (Nalge Nunc International, Naperville, IL) at 1 ml cell suspension/well and transferred to 37°C. After 30 min, samples were placed on ice and processed for 3,3′-diaminobenzidine (DAB)-cross-linking (to preserve the horseradish peroxidase-loaded organelles), permeabilized for 15 min with 40 μg/ml digitonin in permeabilization buffer F (38 mM potassium aspartate, 38 mM potassium gluconate, 38 mM potassium glutamate, 2.5 mM $MgCl_2$, 1.5 mM EGTA, 25 mM HEPES, pH 7.2) and fixed with 2% paraformaldehyde in buffer F all exactly as described previously (Futter *et al*., 1998). Fixed, permeabilized samples were immunolabeled as described by Futter *et al*. (1998) by using the anti-Rab27a antibody 4B12 antibody at 1:100 in 1% BSA in buffer F overnight followed by 10-nm anti-rabbit gold (British Biocell, Cardiff, United Kingdom) at 1:40 in 2% BSA in PBS for 1 h. After immunolabeling, cells were postfixed in 1.5% glutaraldehyde 2% paraformaldehyde in PBS, and processed for 3,3′-diaminobenzidine (DAB)-cytochemistry, postfixed in reduced osmium, and Epon-embedded as described previously (Stinchcombe *et al*., 2001). Semithick (100–400-nm) samples were contrasted with lead citrate and viewed using a 912 Omega Electron Microscope (Carl Zeiss, Thornwood, NY).

RESULTS

Generation of Transgenic Mice Expressing Functional EGFP-Rab27a in Faithful Tissue-specific Pattern

As a tool to study the expression pattern and the role of Rab27a in specialized cell types, we generated a transgenic line of mice expressing EGFP-Rab27a fusion protein under the control of the endogenous Rab27a promoter. To achieve this, we inserted a mini-gene containing EGFP in frame with the Rab27a coding sequence followed by a polyA sequence into the start codon of the *RAB27A* gene isolated on PAC 15798 (Figure 1). PAC 15798 is ~125 kb and carries the 65-kb human *RAB27A* gene flanked by 36 kb of upstream and 8 kb of downstream sequences (Tolmachova *et al*., 1999). The EGFP-Rab27a cDNA was introduced into the PAC 15798 efficiently by GET recombination (Narayanan *et al*., 1999). This strategy allowed the expression of the fusion gene from the endogenous *RAB27A* promoter presumably keeping all enhancers and long-range controlling elements of the gene intact. The *RAB27A* gene on the PAC was disrupted and could not be expressed.

We obtained three independent transgenic mouse lines (FR82, FR84, and FR90), which contained the entire *RAB27A* gene as determined by PCR analysis (Figure 2A). In FR84 and FR90 lines, the pattern of expression of EGFP-Rab27a mimicked that of the endogenous Rab27a, both in terms of tissue specificity and in levels of expression (Figure 2B, see for example brain versus lung expression). These results indicated that the transgene was indeed apparently expressed faithfully.

To test whether the transgenic fusion protein EGFP-Rab27a was functional, we crossed FR84 and FR90 lines with *ashen* (*Rab27a*^{ash}, Rab27a null) mice (Wilson *et al*., 2000) and analyzed the two well established phenotypic characteristics of *ashen* mice, coat color dilution and absent CTL killing activity. In FR90-rescued mice, we observed nearly 100% coat color rescue (Figure 3A), whereas in FR84-rescued mice we observed only partial rescue of the coat color (our unpublished data). In CTLs, killing activity was fully restored in both FR84- and FR90-rescued mice as determined by an in vitro killing assay (Figure 3B). We then isolated and cultured CTLs from FR84-rescued *ashen* mice and then labeled lytic granules with a fluorescent tracer and subjected the cells to time-lapse microscopy. We observed striking colocalization between both fluorescent signals, suggesting that the majority of EGFP-Rab27a protein associated with lytic granules (Movie 1, Supplementary Material). To confirm these findings, we subjected CTLs to immunoelectron microscopy by using anti-Rab27a antibodies and observed that Rab27a localized to the surface of lytic granules (Figure 4). Together, these results demonstrate that the EGFP-Rab27a transgene is both appropriately expressed and functional in FR84 and FR90 lines.

To further investigate the pattern of expression of Rab27a, we subjected mouse tissues to confocal light microscopy. The images shown were obtained using frozen sections as paraffin-embedding obscured EGFP fluorescence. All images shown are merged pictures of sections excited with 488 nm to elicit EGFP-Rab27a fluorescence and 568 nm to elicit intrinsic autofluorescence observed in most tissues. To further ensure the specificity of the EGFP signal, we also subjected tissue sections derived from wild-type mice to fluorescence microscopy and observed either no fluorescence or autofluorescence that could be elicited equally by either 488-nm or 568-nm excitation.

We first observed low to undetectable EGFP-Rab27a fluorescence in the larger organs of the body, namely, the liver, brain, kidney, skeletal muscle, and testis. This is in agreement with our previous immunoblot studies (Seabra *et al*., 1995; Barral *et al*., 2002).

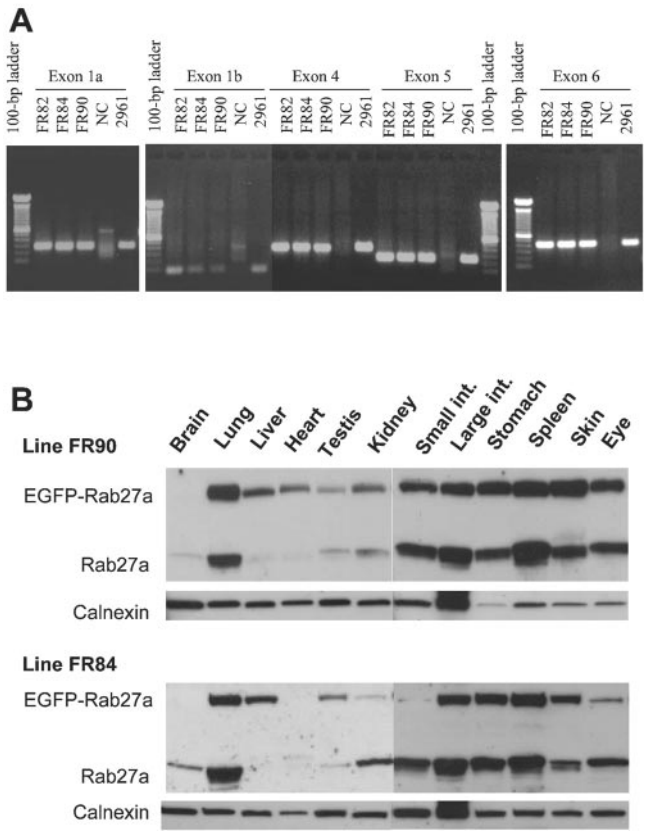

Figure 2. PCR analysis of transgene and expression pattern of EGFP-Rab27a in transgenic lines. (A) PCR analysis of mouse lines with EGFP-Rab27a transgene. DNA isolated from the indicated transgenic founders FR82, FR84, and FR90 was amplified by PCR by using primers specific for sequences outside exons of human *RAB27A* gene described in Table 1. DNA from PAC 2961 was used as a positive control and DNA from a nontransgenic littermate was used as a negative control. (B) Immunoblot analysis of tissues derived from transgenic FR84 and FR90 lines. Tissue protein extracts isolated from the indicated organs were subjected to SDS-PAGE and analyzed by immunoblot by using anti-Rab27a antibody 4B12 and anti-calnexin antibody (as a loading control) as described under MATERIALS AND METHODS.

Rab27a Is Widely Expressed in the Gastrointestinal Tract

Previous studies suggested that Rab27a is expressed in the gastrointestinal tract (Seabra *et al*., 1995; Ramalho *et al*., 2001; Barral *et al*., 2002). Longitudinal sections obtained from the body of the stomach showed that the transgene is highly expressed throughout the gastric glands and pits (Figure 5). Surface mucous cells showed the brightest fluorescence (Figure 5, B and C). Transverse sections demonstrate that the transgene is expressed in the apical region, which is packed with mucigen granules (Figure 5C). Neck mucous cells exhibited clear EGFP signal on the surface of mucigen granules, best observed in the pyloric region (Supplemental Figure S2). The acid-secreting parietal cells were easily noticeable given the presence of highly autofluorescent spots. EGFP-Rab27a staining in parietal cells was thus more difficult to analyze, nevertheless clear EGFP signal was ob-

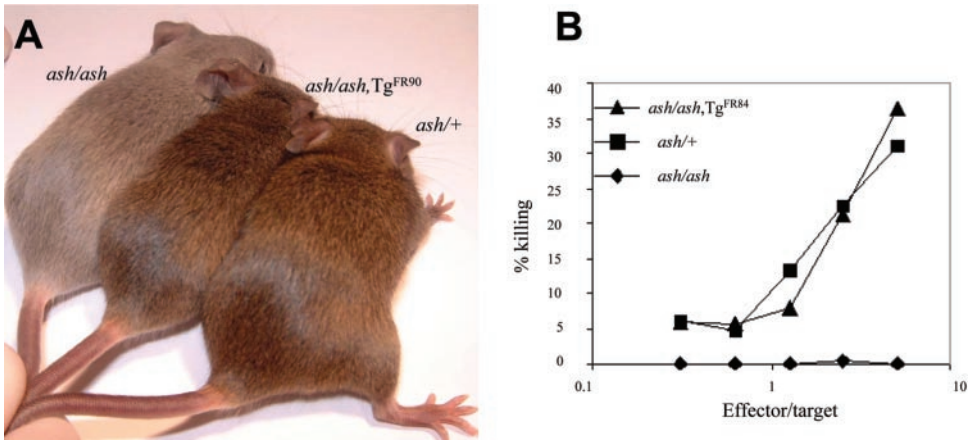

Figure 3. EGFP-Rab27a rescues the phenotype of *ashen* mice. (A) Photograph showing one homozygous *Rab27a*^{ash} mouse (*ash/ash*), one transgenic FR90 homozygous *Rab27a*^{ash} mouse (*ash/ash*,Tg^{FR90}), and one heterozygous *Rab27a*^{ash} mouse (*ash/+*). (B) CTLs derived from homozygous *Rab27a*^{ash} mouse (*ash/ash*) (♦), transgenic FR84 homozygous *Rab27a*^{ash} mouse (*ash/ash*,Tg^{FR84}) (▲), and heterozygous *Rab27a*^{ash} mouse (*ash/+*) (■) were grown and subjected to cytotoxicity assays as described under MATERIALS AND METHODS.

served in a circular, perinuclear pattern (Figure 5D). The pattern of the staining in parietal cells differed along the gland, from more diffuse, net-like circle at the base to a tight bright ring further up in the neck and isthmus region. At the base of the glands, we observed specific staining in groups of cells containing a basally located nucleus and numerous granules observed by phase contrast, consistent with peptic or chief cells (Figure 5D). In these cells, the EGFP signal could be observed in concentric patterns that colocalized with the surface of the granules, as observed by phase contrast. In the pyloric region, a similar pattern emerged (Supplemental Figure S2, E). Intense fluorescence was observed in the more superficial mucous-secreting cells, whereas neck mucous cells and parietal cells were also positive.

Rab27a Is Expressed in Mucin-secreting Cells of Several Organs

Sections of small intestine (duodenum, jejunum, and ileum) exhibited more subtle EGFP-Rab27a staining, consistent with weaker signals on immunoblot analysis. In the epithelial layer, only goblet cells, which were identified by their characteristic shape exhibited significant fluorescence (Figure 6, A and B). Expression in enterocytes was light, if any. In the lamina propria and the core of villi, mononuclear cells (probably leukocytes) stained brightly (Figure 6A). Furthermore, a string-like pattern in the center of villi suggests that EGFP-Rab27a is expressed in lacteal (lymphatic) vessels (Figure 6C). Strong expression of EGFP-Rab27a was found at the bottom of crypts of Lieberkuhn in clusters of cells called Paneth cells, which contain many dense secretory granules (Figure 6, C and D). The EGFP signal colocalized with the surface of the numerous dense granules, which polarize to the luminal side.

Sections of the colon and rectum revealed striking expression in goblet cells, whereas absorptive cells showed little, if any, staining (Figure 6E). High-magnification images of goblet cells from the upper part of the gland revealed that EGFP-Rab27a stained the peripheral rim of the cell and punctate structures within the cytoplasm (Figure 6F, inset). This staining pattern probably represents association of EGFP-Rab27a with the limiting membrane of mucinogen

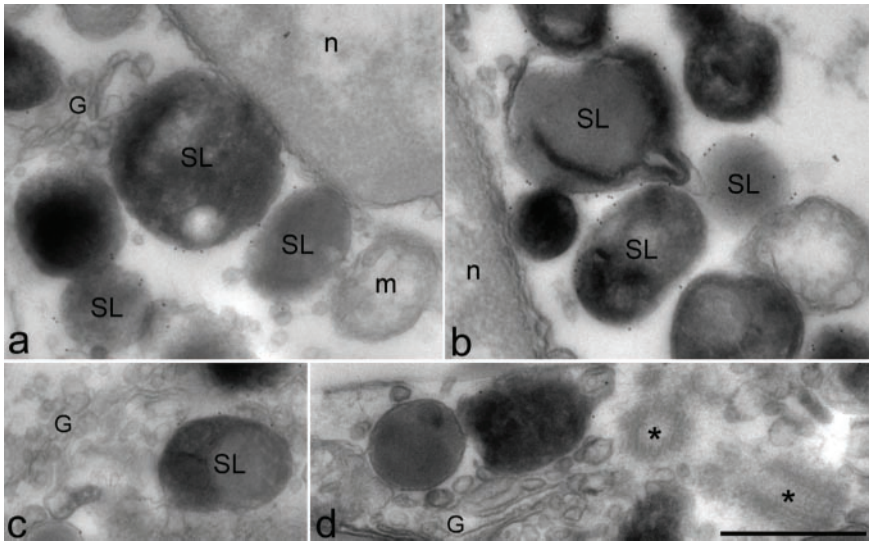

Figure 4. Electron microscopy analysis of CTLs. CTLs derived from FR84-rescued *ashen* mice were subjected to immunoelectron microscopy by using antibodies to Rab27a and gold-labeled anti-mouse secondary antibodies as described under MATERIALS AND METHODS. Antibodies to Rab27a label only the secretory lysosomes (SL), nucleus (n), Golgi (G), mitochondria (m), and the microtubule organizing center (*) are indicated. The four panels depict representative images. Bar, 500 nm.

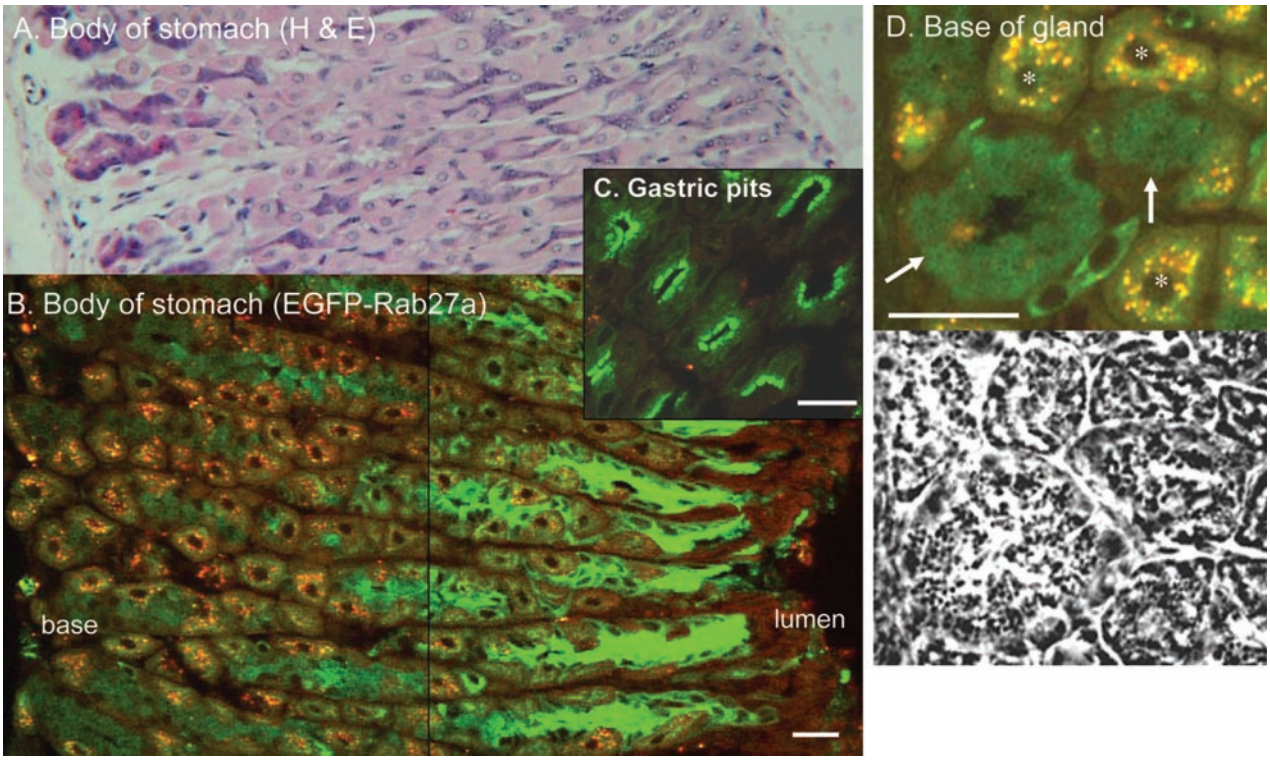

Figure 5. Expression of EGFP-Rab27a transgene in stomach. Frozen sections of the body of the stomach were analyzed using H&E staining (A) and laser confocal microscopy (B–D). Images B–D are merged images obtained with 488- and 568-nm filters where green indicates EGFP fluorescence. (B) Longitudinal cut along gastric pits and glands. (C) Oblique cut through gastric pits. (D) Detail of the base of gastric gland with corresponding phase image below. Arrows show clusters of chief cells and asterisks parietal cells. Note the ring-like pattern of expression of EGFP-Rab27a on the surface of the zymogen granules in chief cells. Bar, 20 μm.

granules, which are very abundant in goblet cells where they fill most of the cell cytoplasm. In addition, it seemed that the EGFP signal colocalized with cytoplasmic dense granules observed by phase contrast (Figure 6F). In the lower part of the gland, goblet cells are also stained but in a distinct apical pattern that resemble the gastric surface mucus-secreting cells (Figure 6E).

The presence of EGFP-Rab27a in mucus-secreting cells was further assessed in the genital and the respiratory tracts. In the uterus, EGFP-Rab27a was present in the apical region of the surface epithelial cells of the endometrium (Supplementary Figure S2). The respiratory tract was more difficult to study. Sections of trachea were unfortunately brightly autofluorescent, preventing an accurate analysis. However, bronchi of different sizes showed fluorescent labeling at the apical region of a subset of cells. In the bronchiole, the apical pattern of staining was more evident in Clara cells (Supplementary Figure S2).

Rab27a Is Expressed in Exocrine Glands

We then studied the expression of EGFP-Rab27a in exocrine glands. EGFP-Rab27a staining was observed in salivary (submaxillary) glands. Both serous and mucous secreting cells as well as cells lining striated ducts exhibited EGFP-Rab27a fluorescence (Figure 7 and Supplemental Figure S2). In serous acinar cells which were identified by the presence of dense zymogen granules, EGFP-Rab27a was present on the surface of the granules in a ring-like pattern, as observed in chief cells (Figure 7A). Mucous acinar cells possessed much paler mucigen granules, which also contained EGFP-Rab27a on their surface (Figure 7A). In striated ducts, EGFP-Rab27a staining was strikingly polarized to the luminal region of the cells (Supplemental Figure S2).

In the exocrine pancreas, EGFP-Rab27a is present in the apical region of the acinar cells, which is rich in zymogen granules (Figure 7B). In sections of the skin, EGFP-Rab27a expression was strikingly evident in sebaceous glands, which secrete into the upper part of the hair follicle (Figure 7C). EGFP-Rab27a was also evident in the basal layers of the epidermis, mostly likely in keratinocytes. Melanocytes are not evident in situ in the skin. Surprisingly, cultures of primary melanocytes derived from both lines exhibited low to undetectable EGFP signal (our unpublished data), which could be due to the combined effects of low expression of EGFP-Rab27a transgene and melanin quenching of fluorescence.

Rab27a Is Expressed in Endocrine Glands

We observed strong EGFP-Rab27a expression in many endocrine glands. We observed significant EGFP labeling of the islet of Langerhans in the pancreas (Figure 8). Immunohistochemistry using anti-glucagon and anti-insulin antibodies to stain α- and β-cells, respectively, suggests that EGFP-Rab27a is expressed in both α- and β-cells (Figure 8). Glucagon-positive α cells exhibited higher levels of EGFP fluorescence than insulin-containing β cells and a characteristic subplasmalemmal location (Figure 8J). The presence of EGFP-Rab27a in β-cells is consistent with recent findings by Izumi and coworkers, who also observed colocalization of Rab27a and insulin (Yi *et al*., 2002).

In sections of the adrenal gland, EGFP-Rab27a was detected in both the medulla and the cortex (Figure 9A). In the

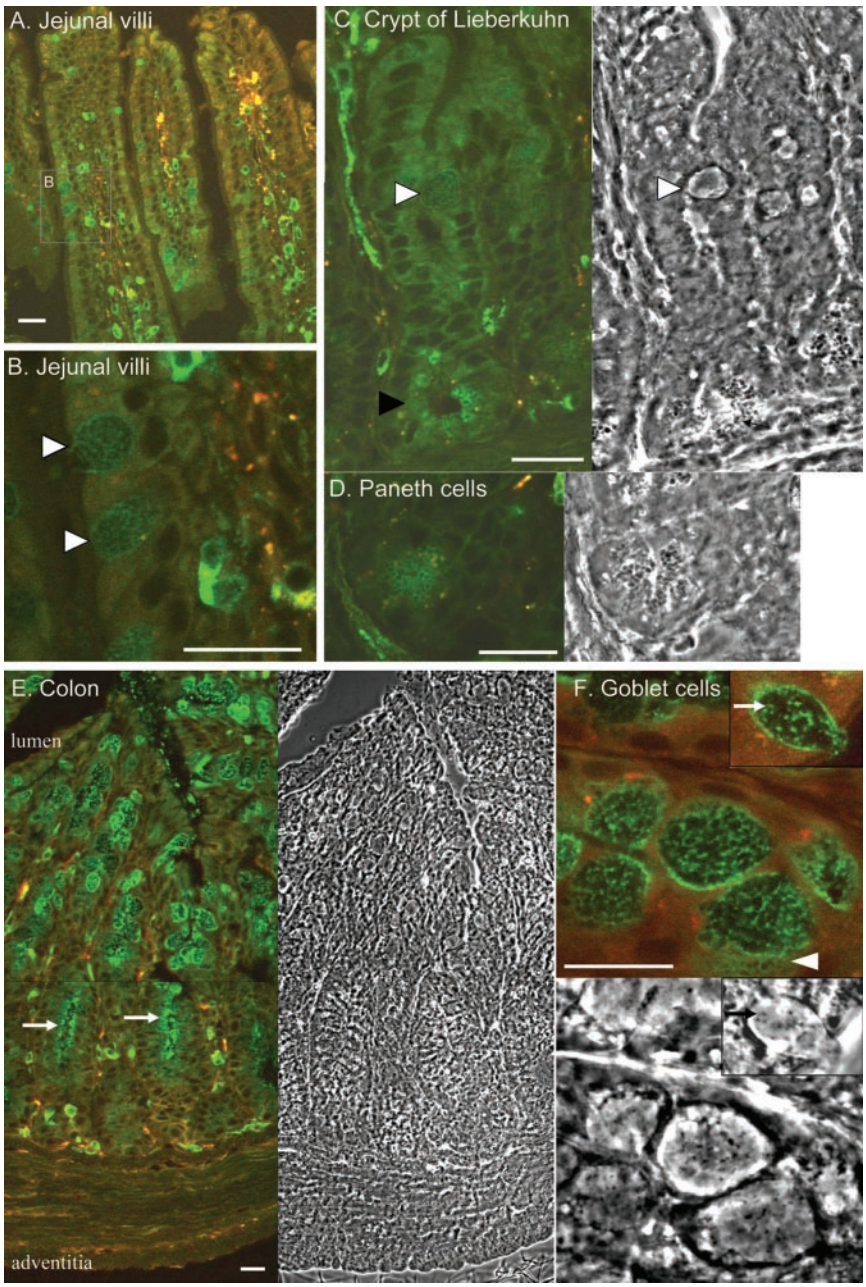

Figure 6. Expression of the EGFP-Rab27a in the intestine. (A) Longitudinal cut along jejunal villi. (B) Enlarged area of image A showing expression of EGFP-Rab27a in goblet cells (open arrowheads). (C) Image of a crypt of Lieberkuhn with corresponding phase image on the right showing expression of EGFP-Rab27a in goblet cells (open arrowhead) and Paneth cells (closed arrowhead). (D) Cluster of Paneth cells at the base of a crypt of Lieberkuhn. Note ring-like expression of EGFP-Rab27a on the surface of the granules. (E) Longitudinal section along the crypts of the colon and corresponding phase image on the right. Note apical localization of EGFP-Rab27a in goblet cells at the bottom of the crypts (arrows). (F) Detail of goblet cells and corresponding phase image below. During cutting of the section some of the mucigen granules were released from the cell (arrowhead), note ring-like EGFP-signal on their surface. Inset picture shows association of EGFP-Rab27a with dense granules (arrow) in goblet cells. Bar, 20 μm.

cortex, EGFP-Rab27a expression was highest in the zona reticularis and less pronounced in the zona fasciculata. The peripheral zona glomerulosa exhibited low, if any, specific staining. In the medulla, we observed two types of cells. One type of cells, which formed clusters and displayed significant autofluorescence, probably corresponds to noradrenaline-secreting cells. The most abundant type cell type, presumably adrenaline-secreting cells exhibited significant EGFP-Rab27a staining (Figure 9A).

The thyroid also exhibited specific EGFP-Rab27a staining. Despite high levels of autofluorescence, EGFP-Rab27a was clearly observed in a polarized distribution closer to the luminal side of the simple cuboidal epithelial cells lining the thyroid follicles (Figure 9B). Finally, disperse endocrine cells of the gastrointestinal tract, which have characteristic positions at the base of the gastric and intestinal glands also expressed EGFP-Rab27a (Figure 9C).

Rab27a Is Expressed in Ovaries and Oocytes

Ovarian sections revealed a surprising pattern of expression for EGFP-Rab27a. In immature follicles, the EGFP signal was clearly observed in the oocyte in a characteristic pattern surrounding the plasma membrane (Figure 10A). In mature follicles, the level of EGFP-Rab27a expression as determined by the intensity of the EGFP signal was much higher, with the protein exhibiting a more diffuse pattern (Figure 10, B and C). Released oocytes were similarly brightly fluorescent (Figure 10D).

To determine whether EGFP-Rab27a was expressed after ovulation and fertilization, we collected fertilized eggs from superovulated EGFP-Rab27a transgenic donors and cultured them in vitro. A representative image showing specific EGFP-Rab27a expression in a four cell-stage embryo is shown in Figure 10E. The levels of fluorescence decreased with time becoming undetectable at blastocyst stage (our unpublished

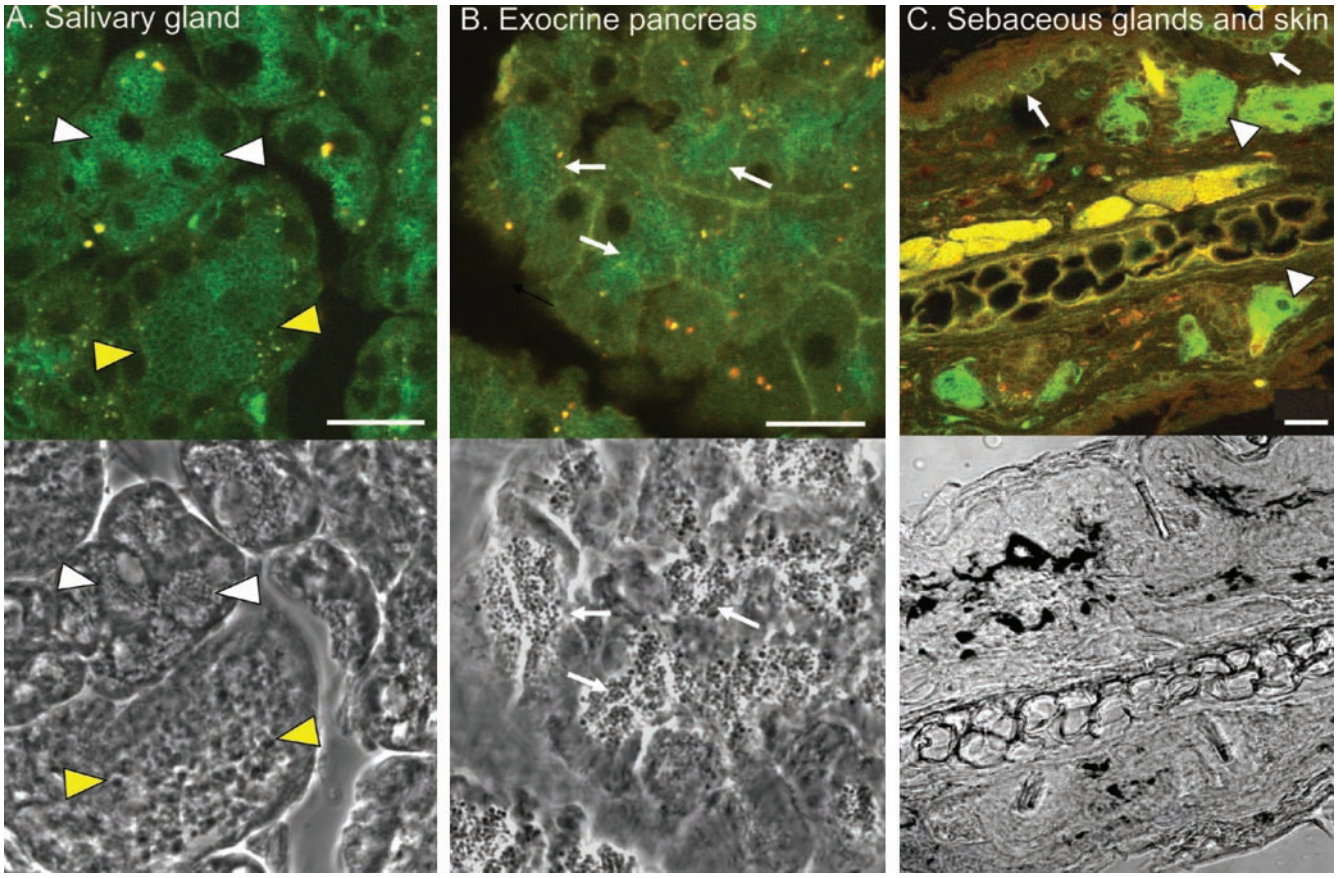

Figure 7. Expression of EGFP-Rab27a in exocrine glands. (A) Section of the submandibular salivary gland with corresponding phase image below showing presence of EGFP-Rab27a on the surface of mucigen granules (white arrowheads) and zymogen granules (yellow arrowheads). (B) Image of acinar cells of the pancreas with corresponding phase image below showing association of EGFP-Rab27a with zymogen granules (arrows). (C) Section of the skin from a mouse ear showing expression of EGFP-Rab27a in sebaceous gland (arrowheads) and basal layer of keratinocytes (arrows). Bar, 20 μm.

data), suggesting that the expression of Rab27a in the early stages of development is maternal rather than embryonic.

Granulosa cells do not seem to express EGFP-Rab27a in either immature or mature follicles; however, granulosa lutein cells exhibited significant expression of EGFP-Rab27a. To further study expression of Rab27a in this cell type, we subjected to light microscopy ovaries derived from mated and nonmated superovulated animals 4.5 d postcoitum. In mated animals, the corpus luteum was round and expressed significant level of EGFP-Rab27a (Figure 10F). In contrast, in superovulated but nonmated females, the corpus luteum was involuting and expression of EGFP-Rab27a was hardly detectable (Figure 10G). The observation that Rab27a is expressed in mature, but not in involuting corpus luteum suggests that expression of Rab27a could be associated with progesterone secretion.

Rab27a^{ash} (Rab27a knockout mice) are fertile despite the striking expression of EGFP-Rab27a in ovaries and oocytes. However, statistical analysis of the reproductive rates in our colonies suggests that the average litter size in *Rab27a*^{ash} is reduced compared with the wild-type background strain (Table 2). Indeed, the average litter size for *Rab27a*^{ash} females in the C57BL/6J background was 50% lower than for C57BL/6J females, whereas for C3H strain the difference in litter size between strains with and without the *ashen* mutation was 20%.

The full list of tissues and cell types where EGFP-Rab27a was detected to date is presented in Table 3.

DISCUSSION

We report the construction of a transgenic mouse model to study the expression and function of Rab27a in specialized membrane trafficking pathways. We produced transgenic mice that express an EGFP-Rab27a fusion protein under the control of the *RAB27A* endogenous promoter leading to faithful cell-type specific expression. Furthermore, we show that the EGFP-Rab27a fusion protein is fully functional as the transgene is able to rescue the two characteristic defects in Rab27a-deficient "*ashen*" mice, namely a coat color dilution and a defect in cytotoxic T-lymphocyte lytic granule exocytosis. Our expression analysis suggests a role for Rab27a in a variety of specialized secretory cell types.

A thorough analysis of the pattern of expression for tissue-specific proteins is usually complicated by the lack of high-affinity and specific antibodies as well as possible artifacts derived from histochemical techniques. Previous studies using Northern and immunoblot analysis suggested the presence of Rab27a in a variety of organs and tissues and a model system in which to study its complex pattern of expression was needed. We created a mouse model faithfully expressing an EGFP-Rab27a fusion protein. We first isolated a PAC contain-

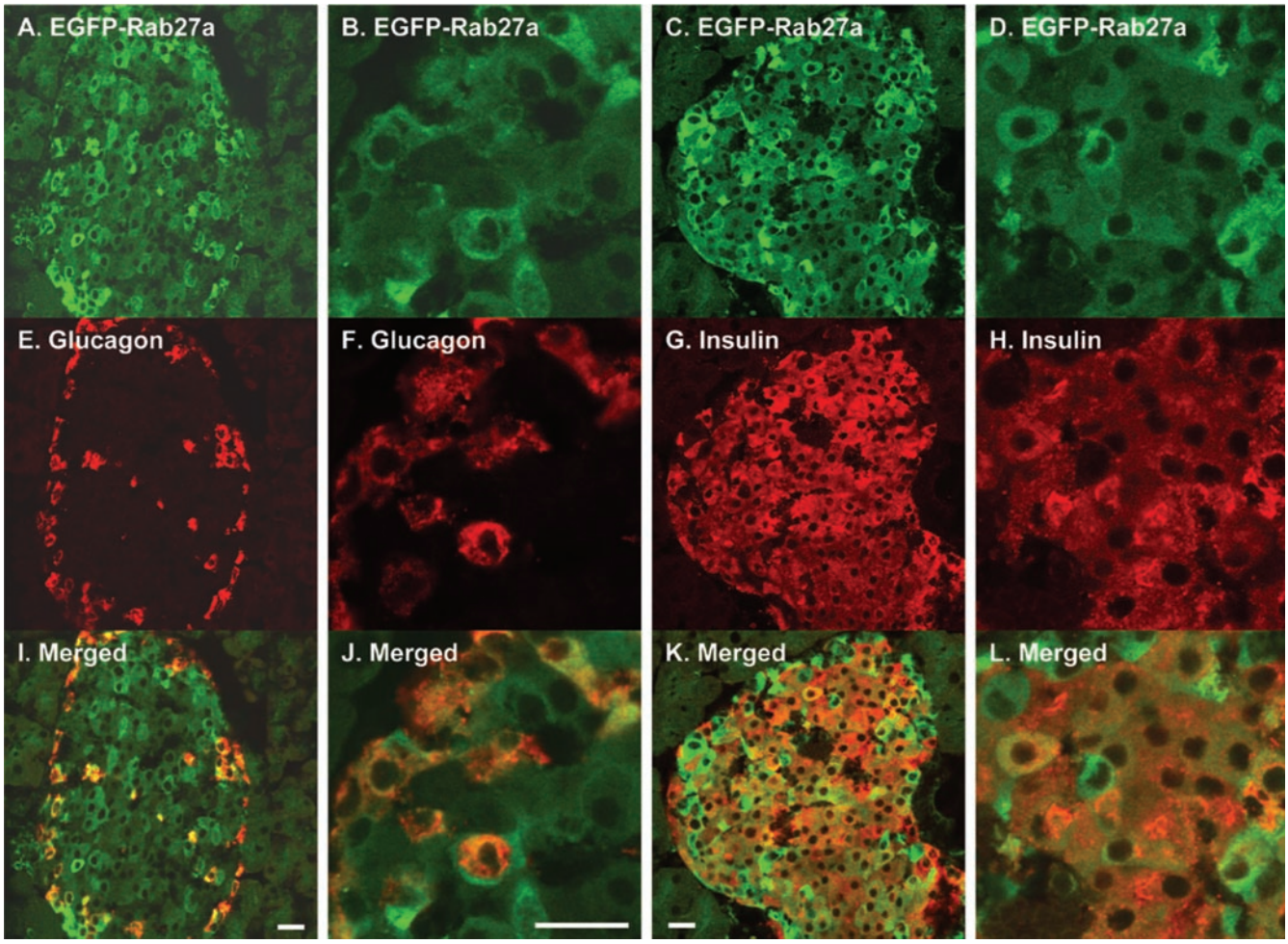

Figure 8. Expression of EGFP-Rab27a in the endocrine pancreas. Frozen sections of mouse pancreas were immunostained with anti-glucagon and anti-insulin antibodies and examined by laser confocal microscopy as described under MATERIALS AND METHODS. (A–D) Fluorescence emission from 488-nm excitation channel. (E–H) Fluorescence emission from 568-nm excitation channel. (I–L) merged images. Bar, 20 μm.

ing the *RAB27A* gene and engineered it such that the promoter would drive the expression of EGFP-Rab27a fusion gene rather than the *RAB27A* gene on the PAC. The recently developed GET recombination system was applied to engineer the PAC and proved to be a highly efficient and precise method for manipulation of large size DNA molecules.

The use of the endogenous promoter allowed us to achieve faithful expression of the transgene. In addition, the use of the PAC as a transgene allowed us to minimize positional effects and variability in expression levels, which is common when a transgene is introduced as a plasmid-based construct. To demonstrate that EGFP-Rab27a was indeed faithfully expressed, we show a comparable pattern of expression between the transgene and the endogenous Rab27a (Figure 2B). Furthermore, we show that the EGFP-Rab27a transgenic protein was functional by generating mice where the transgene was the sole source of Rab27a protein (*ash*/*ash*,Tg). These *ash*/*ash*,Tg mice exhibited wild-type coat color and cytotoxic T cell activity. This is the first demonstration that an EGFP-Rab fusion protein is fully functional in a mammalian organism, in addition to be properly targeted.

Our results suggest a wide role for Rab27a in specialized regulated secretory cells. We found Rab27a expression in a comprehensive range of classic exocrine secretory cells, such as gastric parietal and chief cells, pancreatic acinar cells, sebaceous acinar cells and intestinal Paneth cells (Table 3). EGFP-Rab27a was also present in all tested endocrine cell types, including pancreatic islet cells, adrenal medullary and cortical cells, thyroid follicular cells, and others (Table 3). In most of these cell types, it is noticeable the polarization of Rab27a toward the apical/luminal side of the cell, coinciding with the location of secretory granules. The role of Rab27a in endocrine secretion is not unexpected. Izumi and coworkers proposed a role for Rab27a and its effector granuphilin in insulin secretion from pancreatic β-cells (Yi *et al*., 2002). Furthermore, Fukuda and coworkers suggested a role for Rab27a (and also granuphilin) in secretion from PC12 cells, a model chromaffin cell (Fukuda *et al*., 2002a). Our studies confirm the expression of Rab27a in these cell types and further suggest a general role for Rab27a in exocrine and endocrine exocytosis.

One unexpected observation was the striking correlation between Rab27a expression and mucus secretion. Mucin-secreting cells are particularly abundant in the gastrointestinal tract and Rab27a seems to be highly expressed wherever they occur. The distribution of Rab27a is particularly striking in goblet cells because these exhibit an exuberant abundance of granules. Rab27a is found surrounding the

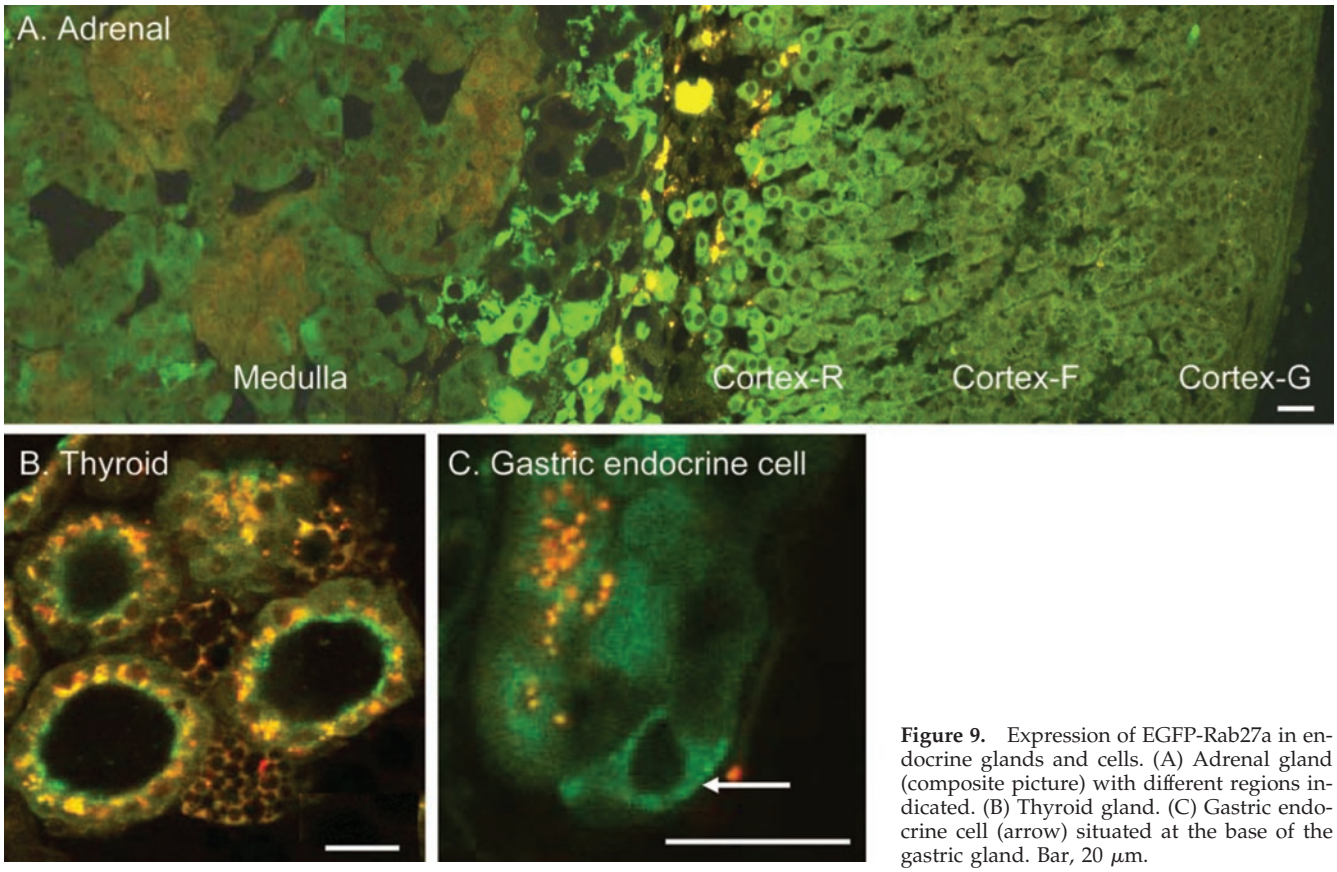

Figure 9. Expression of EGFP-Rab27a in endocrine glands and cells. (A) Adrenal gland (composite picture) with different regions indicated. (B) Thyroid gland. (C) Gastric endocrine cell (arrow) situated at the base of the gastric gland. Bar, 20 μm.

granules filling the small amounts of cytoplasm in the cell, presumably decorating the limiting membrane of mucigen granules. This is observed more clearly in cells containing less granules such as salivary mucus-producing acinar cells. Not much is known about mucin secretion, which seems to be either constitutive or regulated by secretagogues (Rogers, 2003). These seem to be distinct events and regulated secretion involves Ca^{2+}, actin filaments, MARCKS, protein kinase C, and cGMP-dependent protein kinase (McCool *et al*., 1995; Nguyen *et al*., 1998; Li *et al*., 2001).

In addition to exocrine and endocrine cell types, we show here that Rab27a is highly expressed in hematopoietic cells (Table 3). The expression in the former cell types may reflect the presence of lysosome-related organelles (Dell'Angelica *et al*., 2000; Marks and Seabra, 2001; Blott and Griffiths, 2002). So far, Rab27a has been localized to the limiting membrane of melanosomes (Bahadoran *et al*., 2001; Hume *et al*., 2001; Wu *et al*., 2001), CTL lytic granules (this study), platelet α- and δ-granules (Barral *et al*., 2002), and Weibel-Palade bodies (Hannah *et al*., 2003). Our preliminary results suggest that Rab27a is expressed in most other cell types proposed to harbor lysosome-related organelles (Table 3) (D. C. Barral and M. C. Seabra, unpublished data).

One of the most unexpected sites of Rab27a expression is in the ovary. Oocytes exhibit an increasingly high-level expression of Rab27a as they mature. In immature follicules, EGFP-Rab27a distributes to the periphery at or near the plasma membrane. This distribution becomes increasingly diffuse as the level of expression increases with maturation. The released oocyte expresses a striking level of EGFP-Rab27a, which decreases with each cell division in the fertilized oocyte until it is undetectable at the blastocyst stage. These data suggest that the expressed Rab27a is of maternal origin and is not expressed in the very early stages of mouse development. Conversely, granulosa cells do not express significant amounts of EGFP-Rab27a, except after ovulation and mating when they become granulosa lutein cells. Interestingly, mating is required for Rab27a expression in this type of cell (Figure 10, F and G), suggesting a possible role for Rab27a in progesterone secretion. A role for Rab27a in female reproduction is further suggested by our retrospective analysis of the litter size of our mouse colonies. The numbers are low and thus the data remain preliminary (Table 2). Nevertheless, the data suggest that Rab27a knockout mice exhibit low fecundity, and further studies should elucidate more precisely the role of Rab27a in reproductive biology. One interesting hypothesis is that Rab27a could be involved in exocytic events controlled by the oocyte such as cortical granule exocytosis whose function seems to be to block polyspermy during fertilization.

An emerging pattern thus seems to be the expression of Rab27a in a wide range of nonneuronal secretory cells undergoing regulated exocytosis (Table 3). The mechanism of action of Rab27a has been better characterized in melanocytes where it is important for the peripheral myosin Va-driven movement of melanosomes (see INTRODUCTION). The general role of Rab27a in secretory cell types could be to regulate the myosin-dependent movement of secretory vesicles to the vicinity of the plasma membrane. Recent studies suggest a role for myosin V in the movement of secretory granules in chromaffin cells (Rudolf *et al*., 2003). However, the isolation of Rab27 effector proteins containing C2 domains suggest the possibility that Rab27a may have other roles in secretion, including tethering of vesicles to the plasma membrane and/or a participation in

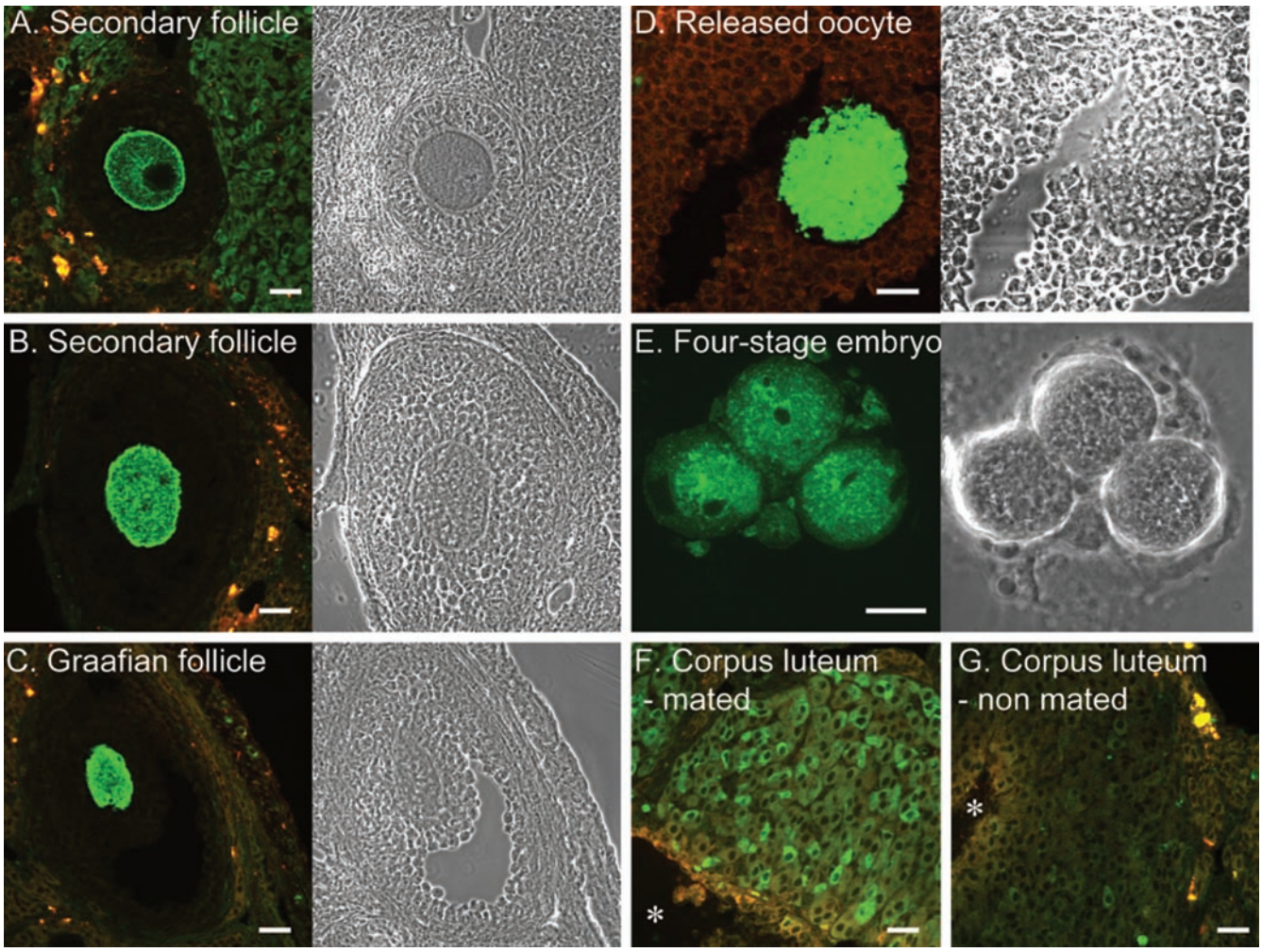

Figure 10. Expression of EGFP-Rab27a in ovary, oocyte, and early embryo. (A) Primary follicle. (B) Secondary follicle. (C) Graafian follicle. (D) Released oocyte. (E) Four cell stage embryo. (F) Corpus luteum from superovulated mated mouse 4.5 d postcoitus. (G). Corpus luteum from superovulated nonmated mouse 4.5 d postcoitus. Postovulatory blood clot is marked with asterisk. For A–E, the corresponding phase contrast image is shown to the right. Bar, 20 μm.

the fusion process (Kuroda *et al*., 2002a; Strom *et al*., 2002; Yi *et al*., 2002). Further experiments to study the involvement of Rab27a in exocytosis are needed.

The results shown here are somewhat surprising given the restricted phenotype observed in loss-of-function mutations in Rab27a found in Griscelli Syndrome. Griscelli Syndrome is a life-threatening disease leading to early lethality in the absence of the bone marrow transplant. The two recognized phenotypic hallmarks of the disease are an exocytosis defect in CTLs and a melanosome transport defect in skin melanocytes. It is possible, indeed likely, that both patients and *ashen* mice suffer from other abnormalities that have remained undetected. However, we have recently shown that the close homolog of Rab27a, Rab27b is able to compensate for the loss-of-function of Rab27a, because transgenic expression of Rab27b rescued coat color dilution in *ashen* mice (Barral *et al*., 2002). The expression pattern of Rab27b seems more restricted, and substantial expression of the protein was detected only in stomach, large intestine, and platelets (Barral *et al*., 2002), raising the possibility that other related Rabs might be able to compensate for the loss of function of Rab27a in tissues where Rab27b is not normally expressed. The Rab3 isoforms, Rab26 and Rab37, form with Rab27 a functional group on the basis of structural homology (Pereira-Leal and Seabra, 2001). Therefore, they represent the best candidates for a compensatory role. Indeed, Rab3D is an especially good candidate for this role, because it is expressed in many exocrine and endocrine tissues similar to the tissues where we found expression of Rab27a (Riedel *et al*., 2002).

The availability of EGFP-Rab27a transgenic mice represents a rich source of cells and tissues to further dissect the role of Rab27a in specialized membrane trafficking path-

Table 2. Effect of *ashen* mutation on the average litter size

Mouse strain	Average litter size (pups/litter)
C57BL/6J (n = 29)	7.17 ± 2.2
C57BL/6J *ashen* (n = 7)	3.43 ± 1.9*
C3H/HeSn (n = 25)	5.00 ± 1.69
C3H/HeSn *ashen* (n = 11)	4.09 ± 1.37

* $P < 0.01$.

Table 3. Tissue- and cell-specific expression of EGFP-Rab27a

Tissue/organ	Cell type	Intracellular distribution	Regulated secretion
Stomach	Parietal cells	Perinuclear	Yes
	Chief cells	Surface of zymogen granules	Yes
	Mucous-secreting cells	Apical region	Yes
	Neck mucous cells	Surface of mucigen granules	
	Enteroendocrine cells	Basal position	Yes
Small intestine	Paneth cells	Surface of apical granules	Yes
	Goblet cells	Surface of mucigen granules	Yes
	Enteroendocrine cells	Basal position	Yes
Large intestine	Goblet cells	Surface of mucigen granules, plasma membrane, dense granules	Yes
Pancreas	Pancreatic acinar cells	Surface of zymogen granules	Yes
	Islet alpha cells	Subplasmalemmal	Yes
	Islet beta cells	Diffuse	Yes
Lung	Pneumocytes type II	Diffuse	Yes
	Clara cells	Subplasmalemmal	Yes
Hyaline cartilage	Chondrocytes	Subplasmalemmal	Yes
Ovary	Oocyte	Diffuse	Yes
	Granulosa lutein cells	Diffuse	
Uterus	Epithelium of endometrium	Apical region	Yes
	Myometrium		
Skin	Basal keratinocytes	Subplasmalemmal	
	Melanocytes[a]		
Sebaceous gland	Sebum-producing acinar cell		Yes
Adrenal gland	Zona reticularis cells	Diffuse	Yes
	Adrenaline-secreting cells	Diffuse	Yes
Thyroid gland	Follicular cells	Apical localisation	Yes
Submandibular gland	Serous secretory cells	Surface of zymogen granules	Yes
	Mucous secretory cells	Surface of mucigen granules	Yes
	Striated ducts epithelium	Apical localisation	Yes
	Myoepithelial cells		
Spleen	Neutrophils[b]	Diffuse	Yes
Lymph node	T-cells	Surface of lytic granules	Yes
Thymus	B-cells[b]		Yes
Bone marrow	Eosinophils[b]	Diffuse	Yes
Blood	Basophils[b]	Diffuse	Yes
	Mast cells[b]	Basophilic granules	Yes

[a] Functional rather than morphological evidence (see Figure 3).

[b] Barral and Seabra (unpublished data).

ways. Movie 1 shows a short-sequence where the endogenous fluorescence of EGFP-Rab27a marks lytic granules in cultured CTLs derived from the transgenic mice. This movie represents an example of the type of experiments now possible. This work combining genetics and cell biology methodologies highlights the complex pattern of expression and function of proteins involved in specialized functions. Because mammalian organisms are composed almost exclusively of highly differentiated cells, such issues will need to be addressed to further our understanding of molecular cell biology and the pathogenesis of human disease.

ACKNOWLEDGMENTS

We thank Jose Ramalho and Duarte Barral for help with mouse work; Lorraine Lawrence and Andrea Robertson for help with histology studies; and B. Wanner, P. Ioannou, Oleg Tolmachov, Brian Bigger, and Alistair Hume for plasmids. This work was supported by the Medical Research Council.

REFERENCES

Bahadoran, P., Aberdam, E., Mantoux, F., Busca, R., Bille, K., Yalman, N., de Saint-Basile, G., Casaroli-Marano, R., Ortonne, J.P., and Ballotti, R. (2001). Rab27a: a key to melanosome transport in human melanocytes. J. Cell Biol. *152*, 843–850.

Barral, D.C., Ramalho, J.S., Anders, R., Hume, A.N., Knapton, H.J., Tolmachova, T., Collinson, L.M., Goulding, D., Authi, K.S., and Seabra, M.C. (2002). Functional redundancy of Rab27 proteins and the pathogenesis of Griscelli syndrome. J. Clin. Investig. *110*, 247–257.

Bigger, B.W., Tolmachov, O., Collombet, J.M., Fragkos, M., Palaszewski, I., and Coutelle, C. (2001). An araC-controlled bacterial cre expression system to produce DNA minicircle vectors for nuclear and mitochondrial gene therapy. J. Biol. Chem. *276*, 23018–23027.

Blott, E.J., and Griffiths, G.M. (2002). Secretory lysosomes. Nat. Rev. Mol. Cell. Biol. *3*, 122–131.

Dell'Angelica, E.C., Mullins, C., Caplan, S., and Bonifacino, J.S. (2000). Lysosome-related organelles. FASEB J. *14*, 1265–1278.

El-Amraoui, A., Schonn, J.S., Kussel-Andermann, P., Blanchard, S., Desnos, C., Henry, J.P., Wolfrum, U., Darchen, F., and Petit, C. (2002). MyRIP, a novel Rab effector, enables myosin VIIa recruitment to retinal melanosomes. EMBO Rep. *3*, 463–470.

Fukuda, M., Kanno, E., Saegusa, C., Ogata, Y., and Kuroda, T.S. (2002a). Slp4-a/granuphilin-a regulates dense-core vesicle exocytosis in PC12 cells. J. Biol. Chem. *277*, 39673–39678.

Fukuda, M., Kuroda, T.S., and Mikoshiba, K. (2002b). Slac2-a/melanophilin, the missing link between Rab27 and myosin Va: implications of a tripartite protein complex for melanosome transport. J. Biol. Chem. *277*, 12432–12436.

Futter, C.E., Gibson, A., Allchin, E.H., Maxwell, S., Ruddock, L.J., Odorizzi, G., Domingo, D., Trowbridge, I.S., and Hopkins, C.R. (1998). In polarized MDCK cells basolateral vesicles arise from clathrin-gamma-adaptin-coated domains on endosomal tubules. J. Cell Biol. *141*, 611–623.

Goud, B. (2002). How Rab proteins link motors to membranes. Nat. Cell Biol. *4*, E77–E78.

Haddad, E. K., Wu, X., Hammer, J. A., 3rd, and Henkart, P. A. (2001). Defective granule exocytosis in Rab27a-deficient lymphocytes from Ashen mice. J. Cell Biol. *152*, 835–842.

Hannah, M.J., Hume, A.N., Arribas, M., Williams, R., Hewlett, L.J., Seabra, M.C., and Cutler, D.F. (2003). Weibel-Palade bodies recruit Rab27 by a content-driven, maturation-dependent mechanism that is independent of cell type. J. Cell Sci. *116*, 3939–3948.

Hogan, B., Bedington, R., Costantini, F., and Lacy, E. (1994). Manipulating the Mouse Embryo: A Laboratory Manual, Cold Spring Harbor, NY: Cold Spring Harbor Laboratory Press.

Hume, A.N., Collinson, L.M., Hopkins, C.R., Strom, M., Barral, D.C., Bossi, G., Griffiths, G.M., and Seabra, M.C. (2002). The leaden gene product is required with Rab27a to recruit myosin Va to melanosomes in melanocytes. Traffic *3*, 193–202.

Hume, A.N., Collinson, L.M., Rapak, A., Gomes, A.Q., Hopkins, C.R., and Seabra, M.C. (2001). Rab27a regulates the peripheral distribution of melanosomes in melanocytes. J. Cell Biol. *152*, 795–808.

Kuroda, T.S., Fukuda, M., Ariga, H., and Mikoshiba, K. (2002a). The Slp homology domain of synaptotagmin-like proteins 1–4 and Slac2 functions as a novel Rab27A binding domain. J. Biol. Chem. *277*, 9212–9218.

Kuroda, T.S., Fukuda, M., Ariga, H., and Mikoshiba, K. (2002b). Synaptotagmin-like protein *5*, a novel Rab27A effector with C-terminal tandem C2 domains. Biochem. Biophys. Res. Commun. *293*, 899–906.

Li, Y., Martin, L.D., Spizz, G., and Adler, K.B. (2001). MARCKS protein is a key molecule regulating mucin secretion by human airway epithelial cells in vitro. J. Biol. Chem. *276*, 40982–40990.

Marks, M.S., and Seabra, M.C. (2001). The melanosome: membrane dynamics in black and white. Nat. Rev. Mol. Cell. Biol. *2*, 738–748.

McCool, D.J., Forstner, J.F., and Forstner, G.G. (1995). Regulated and unregulated pathways for MUC2 mucin secretion in human colonic LS180 adenocarcinoma cells are distinct. Biochem. J. *312*, 125–133.

Menasche, G., *et al*. (2000). Mutations in RAB27A cause Griscelli syndrome associated with haemophagocytic syndrome. Nat. Genet. *25*, 173–176.

Metcalf, W.W., and Wanner, B.L. (1993). Construction of new beta-glucuronidase cassettes for making transcriptional fusions and their use with new methods for allele replacement. Gene *129*, 17–25.

Narayanan, K., Williamson, R., Zhang, Y., Stewart, A.F., and Ioannou, P.A. (1999). Efficient and precise engineering of a 200 kb beta-globin human/bacterial artificial chromosome in E. coli DH10B using an inducible homologous recombination system. Gene Ther. *6*, 442–447.

Nguyen, T., Chin, W.C., and Verdugo, P. (1998). Role of Ca2+/K+ ion exchange in intracellular storage and release of Ca2+. Nature *395*, 908–912.

Pereira-Leal, J.B., and Seabra, M.C. (2001). Evolution of the Rab family of small GTP-binding proteins. J. Mol. Biol. *313*, 889–901.

Pfeffer, S.R. (2001). Rab GTPases: specifying and deciphering organelle identity and function. Trends Cell Biol. *11*, 487–491.

Provance, D.W., James, T.L., and Mercer, J.A. (2002). Melanophilin, the product of the leaden locus, is required for targeting of myosin-Va to melanosomes. Traffic *3*, 124–132.

Ramalho, J.S., Anders, R., Jaissle, G.B., Seeliger, M.W., Huxley, C., and Seabra, M.C. (2002). Rapid degradation of dominant-negative Rab27 proteins in vivo precludes their use in transgenic mouse models. BMC Cell Biol. *3*, 26.

Ramalho, J.S., Tolmachova, T., Hume, A.N., McGuigan, A., Gregory-Evans, C.Y., Huxley, C., and Seabra, M.C. (2001). Chromosomal mapping, gene structure and characterization of the human and murine RAB27B gene. BMC. Genet. *2*, 2.

Riedel, D., *et al*. (2002). Rab3D is not required for exocrine exocytosis but for maintenance of normally sized secretory granules. Mol. Cell. Biol. *22*, 6487–6497.

Rogers, D.F. (2003). The airway goblet cell. Int. J. Biochem. Cell Biol. *35*, 1–6.

Rudolf, R., Kogel, T., Kuznetsov, S.A., Salm, T., Schlicker, O., Hellwig, A., Hammer, J.A., 3rd, and Gerdes, H.H. (2003). Myosin Va facilitates the distribution of secretory granules in the F-actin rich cortex of PC12 cells. J. Cell Sci. *116*, 1339–1348.

Seabra, M.C., Ho, Y.K., and Anant, J.S. (1995). Deficient geranylgeranylation of Ram/Rab27 in choroideremia. J. Biol. Chem. *270*, 24420–24427.

Seabra, M.C., Mules, E.H., and Hume, A.N. (2002). Rab GTPases, intracellular traffic and disease. Trends Mol. Med. *8*, 23–30.

Segev, N. (2001). Ypt and Rab GTPases: insight into functions through novel interactions. Curr. Opin. Cell Biol. *13*, 500–511.

Stinchcombe, J.C., Barral, D.C., Mules, E.H., Booth, S., Hume, A.N., Machesky, L.M., Seabra, M.C., and Griffiths, G.M. (2001). Rab27a is required for regulated secretion in cytotoxic T lymphocytes. J. Cell Biol. *152*, 825–834.

Strom, M., Hume, A.N., Tarafder, A.K., Barkagianni, E., and Seabra, M.C. (2002). A family of Rab27-binding proteins: melanophilin links Rab27a and myosin Va function in melanosome transport. J. Biol. Chem. *277*, 25423–25430.

Tolmachova, T., Ramalho, J.S., Anant, J.S., Schultz, R.A., Huxley, C.M., and Seabra, M.C. (1999). Cloning, mapping and characterization of the human RAB27A gene. Gene. *239*, 109–116.

Wilson, S.M., Yip, R., Swing, D.A., O'Sullivan, T.N., Zhang, Y., Novak, E.K., Swank, R.T., Russell, L.B., Copeland, N.G., and Jenkins, N.A. (2000). A mutation in Rab27a causes the vesicle transport defects observed in ashen mice. Proc. Natl. Acad. Sci. USA *97*, 7933–7938.

Wu, X., Rao, K., Bowers, M.B., Copeland, N.G., Jenkins, N.A., and Hammer, J.A., 3rd. (2001). Rab27a enables myosin Va-dependent melanosome capture by recruiting the myosin to the organelle. J. Cell Sci. *114*, 1091–1100.

Wu, X.S., Rao, K., Zhang, H., Wang, F., Sellers, J.R., Matesic, L.E., Copeland, N.G., Jenkins, N.A., and Hammer, J.A., 3rd. (2002). Identification of an organelle receptor for myosin-Va. Nat. Cell Biol. *4*, 271–278.

Yi, Z., Yokota, H., Torii, S., Aoki, T., Hosaka, M., Zhao, S., Takata, K., Takeuchi, T., and Izumi, T. (2002). The Rab27a/granuphilin complex regulates the exocytosis of insulin-containing dense-core granules. Mol. Cell. Biol. *22*, 1858–1867.

Zerial, M., and McBride, H. (2001). Rab proteins as membrane organizers. Nat. Rev. Mol. Cell. Biol. *2*, 107–117.